Bond-Graph Modeling of 1-D Compressible Flows

Gandolfo, E. F.

Universidad Nacional de Cuyo
Ciudad Universitaria, Parque Gral. San Martín, Mendoza (5500), Argentina
egandolfo@uolsinectis.com.ar

Larreteguy, A. E.

Universidad Argentina de la Empresa
Lima 717, Buenos Aires (1073), Argentina
alarreteguy@uade.edu.ar

Baliño, J. L.

Instituto de Pesquisas Energéticas e Nucleares
Av. Prof. Lineu Prestes 2242, Cidade Universitária, CEP 05508-000, São Paulo, SP, Brazil
jlbalino@net.ipen.br

Abstract— **An application to one-dimensional compressible flows of a general Bond-Graph approach for Computational Fluid Dynamics (BG-CFD), developed in previous papers by the authors, is presented. The shock-tube problem is modeled and simulated by this novel approach, and the results are compared against the available analytical solution. The numerical simulation shows that, even with the simple shape and weight functions selected for this case, the BG-CFD approach is able to deal with really complex non-linear flow problems in which all the thermodynamic aspects are taken into account.**

Keywords: **Bond Graphs, Computational Fluid Dynamics, compressible flow, shock tube.**

I. Nomenclature

c	specific heat
C_{av}	artificial viscosity coefficient
h	enthalpy, also length of 1D domain
$\mathbf{I}$	identity matrix
k_θ	coefficient of isothermal compressibility
K	kinetic co-energy per unit mass
M	system inertia
m	mass
n	number of nodes, also time step index
P	pressure
$\mathbf{R}$	rate of deformation
S	entropy
s	specific entropy
u	specific internal energy
V	fluid velocity
t	time
w	weight function
x	position
α	coefficient of thermal expansion
β	numerical parameter
δ	Kronecker delta, also Dirac's function
Δt	time step
λ	thermal conductivity
Γ	domain boundary
Ω	volume, domain
Φ	volumetric heat source
ϕ	interpolation function
Ψ	Gibbs free energy per unit mass
ρ	density
τ	viscous stress tensor
Θ	temperature (nodal)
θ	temperature
μ	dynamic viscosity
Sub or	**Supraindices**
n, k	time indices
m, n	spatial indices
k, l, n	nodal indices
s, V, ρ	pertaining to entropy, velocity, or density
v	per unit volume

II. Introduction

In order to solve multidimensional problems with the aid of computer programs, it is important that these models can be implemented numerically. This task, main concern of the area of Computational Fluid Dynamics (CFD), is performed by systematically discretizing the continua, that is, by replacing the continuous variables by a combination of a finite set of nodal values and interpolating functions. The result is a (generally nonlinear) algebraic approximation, instead of the original differential or integro-differential problem.

The Bond-Graph formalism allows for a systematic approach for representing and analyzing dynamic systems [1]. Dynamic systems belonging to different fields of knowledge, like Electrodynamics, Solid Mechanics, Fluid Mechanics, etc., can be described in terms of a finite number of variables and basic elements. Bond-Graph modeling procedures reported in the literature start from lumped-parameter systems, so integration in space and also assumptions related to the resolution scheme are made beforehand.

In recent works [2][3], a theoretical development of a general Bond-Graph approach for CFD, which we shall

call BG-CFD, was presented. Density, entropy per unit volume and velocity were used as discretized variables; in this way, time-dependent nodal values and interpolation functions were introduced to represent the flow field. Nodal vectors were defined as Bond-Graph state variables, namely mass, entropy and velocity. It was shown that the system total energy can be represented as a 3-port IC field. The conservation of linear momentum for the nodal velocity is represented at the inertial port, while mass and entropy conservation equations are represented at the capacitive ports. All kind of boundary conditions are handled consistently and can be represented either as generalized modulated effort sources at the inertial port or modulated flow sources at the capacitive ports.

In [4][5], the BG-CFD approach was successfully applied to one-dimensional convection-diffusion problems. The "upwind " nature of the fluid equations was naturally handled through the definition of density and entropy weight functions, which share the importance of different power terms among neighboring nodes.

In a separate paper presented at this Conference [6], it is shown that the BG-CFD is a very general methodology, which includes the well-known Control-Volume and Finite-Difference methods as particular cases.

As far as the authors know, the first application of Bond Graphs to CFD problems appeared in [7], although the formulation was restricted to prescribed shape functions and nodalization. Besides, heat conduction (which leads to convection-diffusion problems) was not modeled.

In this paper, the BG-CFD formalism is applied to one-dimensional compressible flows. The general theory is not repeated here, so the readers are encouraged to consult the references for further details.

The rest of the paper is organized as follows. First, the general Bond-Graph equations for compressible flows with heat transfer are presented. The next sections are devoted to describe the numerical details of the discretization. Finally, numerical results for the shock-tube problem are compared against analytical solutions.

In the following, bold letters will be used to define first order tensors (e.g. $\boldsymbol{V}$, $\boldsymbol{p}_v$). Column vectors associated to nodal values will be denoted by single underscored plain or bold type (e.g. $\underline{m}$, $\underline{S}$, $\underline{\boldsymbol{V}}$, $\underline{\varphi_\rho}$, etc.) while multidimensional matrices will be identified by double underscored plain type (e.g. $\underline{\underline{M}}$, $\underline{\underline{\Omega_\rho}}$, etc.). Second order tensors will be denoted by bold, double underscored type (e.g. $\underline{\underline{\boldsymbol{\tau}}}$, $\underline{\underline{\mathbf{I}}}$). Einstein convention of summation over repeated indices is *not* used.

III. System Bond Graph and State Equations

The general system Bond Graph is shown in Fig. 1. A modulated transformer with transformation matrix equal to the inertia matrix, $\underline{\underline{M}}$, is connected to the inertial port of the IC field, in order to bring the nodal velocities as generalized flow variables.

At the 1-element with common nodal velocities, $\underline{\boldsymbol{V}}$, we add all the nodal vector forces; in this way, the effort balance represents the linear momentum conservation equation for the nodal velocity values.

At the 0-element with common nodal kinetic coenergy and Gibbs free energy per unit mass, respectively $(\underline{\Psi} + \underline{K})$, we add all the nodal mass changes per unit time; in this way, the flow balance represents the mass conservation equations for the nodal mass values.

At the 0-element with common nodal temperature, $\underline{\Theta}$, we add all the nodal entropy changes per unit time; in this way, the flow balance represents the thermal energy conservation equation for the nodal entropy values.

The modulated transformers and the modulated gyrator connect power terms that appear in the balance equations corresponding to more than one IC port. Their coupling matrices are rectangular, setting a restriction in the allowable causalities.

The system state equations can be readily obtained from inspection of the system Bond Graph:

$$\underline{\dot{m}} = -\underline{\dot{m}_{WF}} - \underline{\dot{m}_W^{(\Gamma)}} + \underline{\dot{m}_C} + \underline{\dot{m}_P} + \underline{\dot{m}_K} \qquad (1)$$

$$\underline{\dot{\boldsymbol{V}}} = \underline{\underline{M}}^{-1} \cdot \left(\underline{\boldsymbol{F}_G} + \underline{\boldsymbol{F}_T^{(\Gamma)}} - \underline{\boldsymbol{F}_D} - \underline{\boldsymbol{F}_P} - \underline{\boldsymbol{F}_K} \right) \qquad (2)$$

$$\underline{\dot{S}} = \underline{\dot{S}_{QF}} + \underline{\dot{S}_Q^{(\Gamma)}} + \underline{\dot{S}_F} - \underline{\dot{S}_C} + \underline{\dot{S}_D} \qquad (3)$$

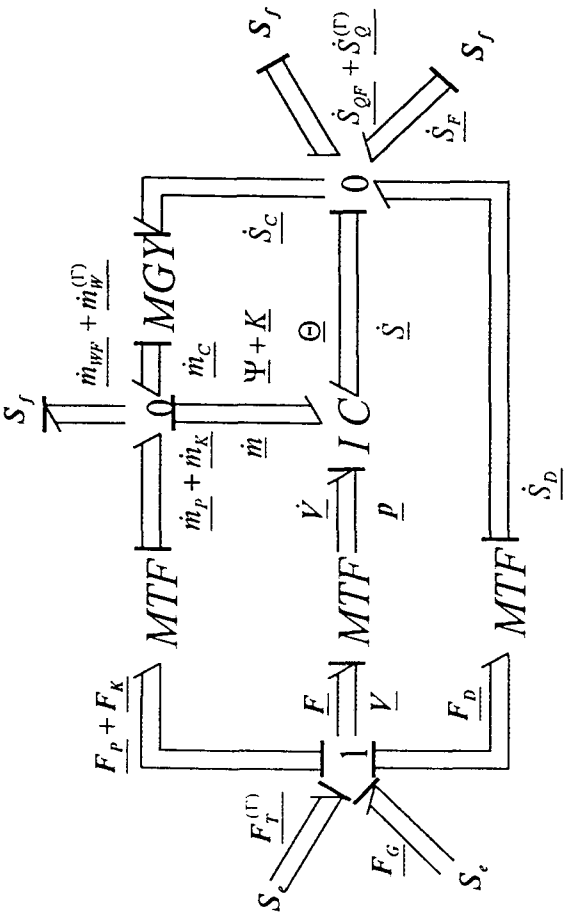

Fig. 1. System Bond Graph

Modulated sources are needed to represent the different boundary conditions established in the problem ($\underline{\dot{m}_W^{(\Gamma)}}$, $\underline{F_T^{(\Gamma)}}$ and $\underline{\dot{S}_Q^{(\Gamma)}}$), as well as to represent the volumetric sources $\underline{\dot{m}_{WF}}$ and $\underline{\dot{S}_{QF}}$. In Eq. (2), $\underline{\underline{M}}$ is the system inertia matrix (symmetric and regular), defined as

$$\underline{\underline{M}} = (M)_{mn} = \int_\Omega \rho\, \varphi_{Vm}\, \varphi_{Vn}\, d\Omega \tag{4}$$

The different terms in the system state equations (1) to (3) arise from integrations over the domain Ω or the domain boundary Γ. Their definition follows.

$$\underline{\dot{m}_{WF}} = \frac{-1}{\underline{\underline{\Psi}} + \underline{\underline{K}}} \cdot \int_\Omega \rho (h + \kappa)\ \boldsymbol{V}.\nabla \underline{w_\rho} d\Omega \tag{5}$$

$$\underline{\dot{m}_W^{(\Gamma)}} = \frac{1}{\underline{\underline{\Psi}} + \underline{\underline{K}}} \cdot \int_\Gamma \underline{w_\rho}\ \rho\ (h + \kappa)\ \boldsymbol{V}.\check{\mathbf{n}}\, \mathbf{d\Gamma} \tag{6}$$

$$\underline{\dot{m}_C} = \frac{1}{\underline{\underline{\Psi}} + \underline{\underline{K}}} \cdot \int_\Omega \underline{w_\rho}\ \theta\ \nabla.(s_v\ \boldsymbol{V})\ d\Omega \tag{7}$$

$$\underline{\dot{m}_P} = \frac{1}{\underline{\underline{\Psi}} + \underline{\underline{K}}} \cdot \int_\Omega \underline{w_\rho}\ \nabla P\ .\ \boldsymbol{V}\ d\Omega \tag{8}$$

$$\underline{\dot{m}_K} = \frac{1}{\underline{\underline{\Psi}} + \underline{\underline{K}}} \cdot \int_\Omega \underline{w_\rho}\ \rho\ \nabla \kappa\ .\ \boldsymbol{V}\ d\Omega \tag{9}$$

$$\underline{\boldsymbol{F}_G} = \int_\Omega \rho\, \boldsymbol{G}\, \underline{\varphi_V}\, d\Omega \tag{10}$$

$$\underline{\boldsymbol{F}_T^{(\Gamma)}} = \int_\Gamma \left(\underline{\underline{\tau}}\ .\ \check{\mathbf{n}}\right)\ \underline{\varphi_V}\ d\Gamma \tag{11}$$

$$\underline{\boldsymbol{F}_D} = \int_\Omega \underline{\underline{\tau}}\ .\ \nabla \underline{\varphi_V}\ d\Omega \tag{12}$$

$$\underline{\boldsymbol{F}_P} = \int_\Omega \nabla P\ \underline{\varphi_V}\ d\Omega \tag{13}$$

$$\underline{\boldsymbol{F}_K} = \int_\Omega \rho\ \nabla \kappa\ \underline{\varphi_V}\ d\Omega \tag{14}$$

$$\underline{\dot{S}_{QF}} = \underline{\underline{\Theta}}^{-1} \cdot \int_\Omega \boldsymbol{q}\ .\ \nabla \underline{w_s}\ d\Omega \tag{15}$$

$$\underline{\dot{S}_Q^{(\Gamma)}} = -\underline{\underline{\Theta}}^{-1} \cdot \int_\Gamma \underline{w_s}\ \boldsymbol{q}\ .\ \check{\mathbf{n}}\ \mathbf{d\Gamma} \tag{16}$$

$$\underline{\dot{S}_F} = \underline{\underline{\Theta}}^{-1} \cdot \int_\Omega \underline{w_s}\ \Phi\ d\Omega \tag{17}$$

$$\underline{\dot{S}_C} = \underline{\underline{\Theta}}^{-1} \cdot \int_\Omega \underline{w_s}\ \theta\ \nabla.(s_v\ \boldsymbol{V})\ d\Omega \tag{18}$$

$$\underline{\dot{S}_D} = \underline{\underline{\Theta}}^{-1} \cdot \int_\Omega \underline{w_s}\ \left(\nabla \boldsymbol{V} : \underline{\underline{\tau}}\right)\ d\Omega \tag{19}$$

The continuous variables ρ, $\boldsymbol{V}$, and s_v are respectively the density, the fluid velocity, and the entropy per unit volume; the potentials κ, ψ, and θ are correspondingly the kinetic coenergy and Gibbs free energy per unit mass and the temperature; t is the time, $\boldsymbol{q}$ is the heat flux, P is the pressure, $\boldsymbol{G}$ is the force per unit mass, $\underline{\underline{\tau}}$ is the viscous stress tensor, Φ is the volumetric heat source and $h = \frac{1}{\rho}\ (u_v + P)$ is the enthalpy per unit mass, where u_v is the internal energy per unit volume.

The heat flux $\boldsymbol{q}$, the pressure gradient, and the viscous stress tensor $\underline{\underline{\tau}}$ (for a Newtonian fluid under Stoke's hypothesis) can be expressed in terms of the continuous variables as:

$$\boldsymbol{q} = -\frac{\lambda\, \theta}{\rho\, c_v} \left[\nabla s_v + \frac{1}{\rho} \left(\frac{\alpha}{\kappa_\theta} - s_v\right)\ \nabla \rho\right] \tag{20}$$

$$\nabla P = \frac{\theta}{\rho\, c_v}\ \frac{\alpha}{\kappa_\theta} \left[\nabla s_v + \left(\frac{c_v}{\alpha\ \theta} + \frac{\alpha}{\rho \kappa_\theta} - \frac{s_v}{\rho}\right) \nabla \rho\right] \tag{21}$$

$$\underline{\underline{\tau}} = \mu\ \left(\nabla \boldsymbol{V} + \nabla \boldsymbol{V}^T\right) - \frac{2}{3}\ \mu\ (\nabla.\boldsymbol{V})\ \underline{\underline{\mathrm{I}}} \tag{22}$$

where λ is the thermal conductivity, c_v is the constant volume specific heat, α is the coefficient of thermal expansion, κ_θ is the coefficient of isothermal compressibility, and μ is the fluid viscosity.

With the introduction of appropriate (see [2]) nodal shape functions for density, velocity, and entropy, namely $\underline{\varphi_\rho}$, $\underline{\varphi_V}$, and $\underline{\varphi_s}$ we define nodal vectors of integrated variables. The nodal vectors of integrated mass and entropy appearing in Eqs. (1) and (3) are:

$$\underline{m} = \underline{\underline{\Omega_\rho}} \cdot \underline{\rho} \tag{23}$$

$$\underline{S} = \underline{\underline{\Omega_s}} \cdot \underline{s_v} \tag{24}$$

where the diagonal matrices $\underline{\underline{\Omega_\rho}}$ and $\underline{\underline{\Omega_s}}$ are

$$\underline{\underline{\Omega_\rho}} = (\Omega_\rho)_{kn} = \int_\Omega \varphi_{\rho k}\ \delta_{kn}\ d\Omega \tag{25}$$

$$\underline{\underline{\Omega_s}} = (\Omega_s)_{ln} = \int_\Omega \varphi_{sl}\ \delta_{ln}\ d\Omega \tag{26}$$

where $\underline{\underline{\delta}}$ is the Kronecker delta.

The vectors of nodal potentials are:

$$\underline{K}\ (\underline{\boldsymbol{V}}) = \underline{\underline{\Omega_\rho}}^{-1} \cdot \left[\int_\Omega \kappa\ \underline{\varphi_\rho}\ d\Omega\right] \tag{27}$$

$$\underline{\Theta}\ (\underline{S},\ \underline{m}) = \underline{\underline{\Omega_s}}^{-1} \cdot \left[\int_\Omega \theta\ \underline{\varphi_s}\ d\Omega\right] \tag{28}$$

$$\underline{\Psi}\ (\underline{S},\ \underline{m}) = \underline{\underline{\Omega_\rho}}^{-1} \cdot \left[\int_\Omega \psi\ \underline{\varphi_\rho}\ d\Omega\right] \tag{29}$$

For the sake of convenience, we also define the following diagonal matrices, whose diagonal elements are the components of the vectors of nodal potentials $\underline{\Theta}$, $\underline{\Psi}$ and $\underline{K}$:

$$\underline{\underline{\Theta}} = (\Theta)_{ln} = \Theta_l\ \delta_{ln} \tag{30}$$

$$\underline{\underline{\Psi}} = (\Psi)_{kn} = \Psi_k\ \delta_{kn} \tag{31}$$

$$\underline{\underline{K}} = (K)_{kn} = K_k\ \delta_{kn} \tag{32}$$

Appropriate weight functions for density and entropy, namely $\underline{w_\rho}$ and $\underline{w_s}$, are also required for the discretization to share the different terms appearing in the mass and entropy port balances, eqs.(1) and (3), among the neighboring nodes. Note that weight functions for velocity are not required.

IV. Numerical Model for 1D Problems

In this section we apply the formalism to one-dimensional compressible flows. We start by defining $n_s = n_\rho = nv$ equidistant nodes in the domain $\Omega = [0, h]$. We chose the density, velocity, and entropy nodes to be coincident, although this is not required by the general formalism. Secondly, we define a particular set of interpolating and weight functions that we found are suitable for dealing with this type of flows. Finally, using this set we obtain a complete numerical model of the problem.

A. Entropy Shape and Weight Functions

For an inner node ($1 < l < n_\rho$), we consider the following entropy shape and weight functions:

$$\varphi_{sl} = \begin{cases} 0 & x < -\frac{h}{2} \\ 1 & -\frac{h}{2} < x < \frac{h}{2} \\ 0 & x > \frac{h}{2} \end{cases} \tag{33}$$

$$w_{sl} = \begin{cases} 0 & x \le -h \\ 1 + \frac{x}{h} + \beta & -h < x < 0 \\ 1 & x = 0 \\ 1 - \frac{x}{h} - \beta & 0 < x < h \\ 0 & x \ge h \end{cases} \tag{34}$$

In Eq. (33) and (34), x is a local coordinate with origin at the entropy node l, as shown in Fig. 2. In Eq. (34), β is a local parameter, which must be optimized in order to satisfy a specified condition, regarding the accuracy of the numerical solution. The analysis for this optimization can be found in [4][5]. In this case, it is used to apply some "upwinding" to the resulting discretization.

It is important to notice that, for the chosen shape function, the element S_l of the entropy vector can be thought as the entropy corresponding to a "control volume" located at $-\frac{h}{2} \le x \le \frac{h}{2}$. Besides, the shape function is discontinuous at $x = -\frac{h}{2}$ and $x = +\frac{h}{2}$, while (for $\beta \neq 0$) the weight function is discontinuous at $x = -h$, $x = 0$ and $x = h$. From Eqs. (33) and (34) we get:

$$\frac{\partial \varphi_{sl}}{\partial x} = \delta\left(x + \frac{h}{2}\right) - \delta\left(x - \frac{h}{2}\right) \tag{35}$$

where $\delta(x)$ is the Dirac's delta function.

$$\frac{\partial w_{sl}}{\partial x} = \begin{cases} 0 & x < -h \\ \beta\,\delta(x+h) & x = -h \\ \frac{1}{h} & -h < x < 0 \\ -2\,\beta\,\delta(x) & x = 0 \\ -\frac{1}{h} & 0 < x < h \\ \beta\,\delta(x-h) & x = h \\ 0 & x > h \end{cases} \tag{36}$$

Since:

$$\frac{\partial s_v}{\partial x} = \sum_{l=1}^{n_s} s_{vl}\,\frac{\partial \varphi_{sl}}{\partial x} \tag{37}$$

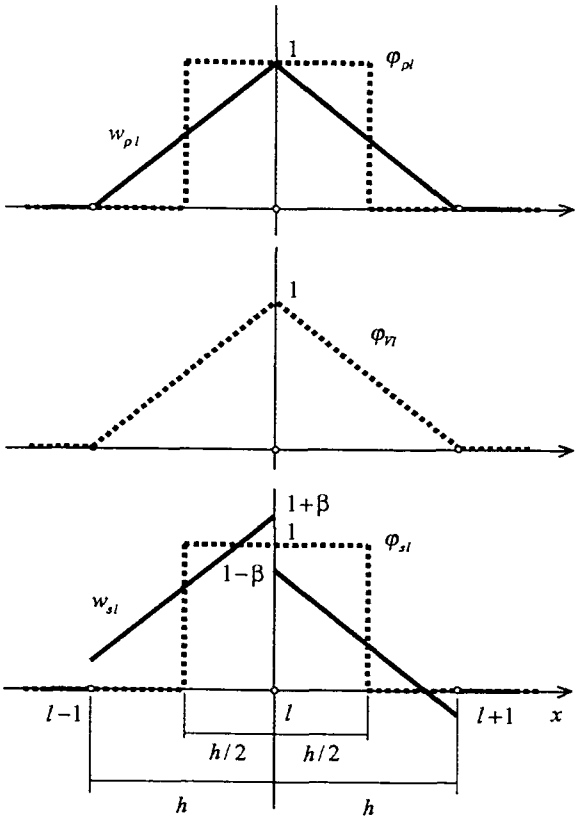

Fig. 2. Shape and weight functions

and taking into account Eq. (35) we have, for $-h \le x \le h$:

$$\frac{\partial s_v}{\partial x} = (s_{v\,l} - s_{v\,l-1})\;\delta\left(x + \frac{h}{2}\right) + (s_{v\,l+1} - s_{v\,l})\;\delta\left(x - \frac{h}{2}\right) \tag{38}$$

Boundary points are treated similarly, but considering only half of a control volume.

B. Density Shape and Weight Functions

For density, we chose the same shape and weight functions than for entropy, except that upwinding is not applied. That is:

$$\varphi_{\rho l}(x) = \varphi_{sl}(x) \tag{39}$$

$$w_{\rho l}(x) = w_{sl}(x|\beta = 0) \tag{40}$$

Again, boundary points are treated similarly, but considering only half of a control volume.

C. Velocity Shape Functions

In this case, we chose for the velocity *shape* functions, a piecewise linear function coincident with the density *weight* functions, that is:

$$\varphi_{vl}(x) = w_{\rho l}(x) \tag{41}$$

As in the previous cases, boundary points are treated by considering only half of a control volume.

D. Numerical Model

Introducing the so defined shape and weight functions into the nodal mass and entropy rate vectors and into the nodal force vectors, and replacing the resulting terms in the system state equations (1-3), we are able to compute the time derivatives of the three integrated nodal vectors in terms of the nodal values of the variables, that is:

$$\underline{\dot{m}} = \underline{\dot{m}}(\underline{\rho}, \underline{V}, \underline{s_v}) \tag{42}$$

$$\underline{\dot{V}} = \underline{\dot{V}}(\underline{\rho}, \underline{V}, \underline{s_v}) \tag{43}$$

$$\underline{\dot{S}} = \underline{\dot{S}}(\underline{\rho}, \underline{V}, \underline{s_v}) \tag{44}$$

It is worth noting that, for a the currently selected shape and weight functions, for given $\underline{\rho}, \underline{V}$ and $\underline{s_v}$, the vectors $\underline{\dot{m}}$ and $\underline{\dot{S}}$ can be computed element by element, while the vector $\underline{\dot{V}}$ requires the inversion of the tridiagonal matrix $\underline{\underline{M}}$ in order to be solved for.

Discretizing time to a first order approximation, we get a (possibly non-linear) algebraic system of equations of the form:

$$\underline{m}^{n+1} = \underline{m}^n + \Delta t\ \underline{\dot{m}}(\underline{\rho}^k, \underline{V}^k, \underline{s_v}^k) \tag{45}$$

$$\underline{V}^{n+1} = \underline{V}^n + \Delta t\ \underline{\dot{V}}(\underline{\rho}^k, \underline{V}^k, \underline{s_v}^k) \tag{46}$$

$$\underline{S}^{n+1} = \underline{S}^n + \Delta t\ \underline{\dot{S}}(\underline{\rho}^k, \underline{V}^k, \underline{s_v}^k) \tag{47}$$

where the subscript n indicates past (known) values at the previous time step, $n+1$ indicates present (to be found) values, and k indicates any time in the interval $[t^n - t^{n+1}]$. If $k = n$ the time approximation is explicit, and the solution of the algebraic system is straightforward. In any other case, the time approximation is implicit, and iteration is required inside each time step.

V. Test Problem: The Shock Tube

The numerical model has been validated against a one-dimensional shock-tube problem for which an analytical solution is known [8]. The problem is depicted in Figure 3. The tube of unit length and a cross section of 0.01 m^2, has been discretized into 100 equal sections, which means $n_s = nV = n_\rho = 101$ equally spaced nodes. No-flow and adiabatic boundary conditions were specified at both ends. The following fluid properties for air (taken from [7]) were used:

- reference temperature $\theta_0 = 273.0\ K$.
- reference density $\rho_0 = 1.2955\ kg\ m^{-3}$.
- constant viscosity $\mu = 1.7153 \times 10^{-5}\ Pa\ s$.
- constant volume specific heat $c_v = 718.0\ J\ kg^{-1}\ K^{-1}$.

The domain is initially separated in two sections by a solid wall located at $x = 0.5\ m$. The gas is at rest in both sections, and the density and total entropy conditions are:

- left section: $\rho = \rho_0$, $S = 0.0\ J\ K^{-1}$.
- right section: $\rho = \rho_0/2$, $S = 4.4247\ J\ K^{-1}$.

At $t = 0$ the solid wall is ruptured, causing a shock wave that travels from left to right.

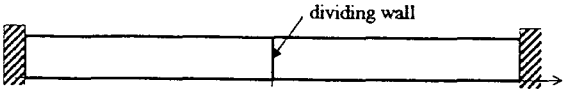

Fig. 3. The Shock-Tube Problem.

The algebraic system of equations was solved explicitly, with a time step of $1.3 \times 10^{-5}\ s$. As is usually suggested ([7],[9],[10]), an artificial viscosity μ_a was introduced, in the following way:

$$\mu_a = \mu \left[1.0 + C_{av}\ \frac{1}{2}\ tr\ (\underline{\underline{\mathbf{R}}}^2)\right] \tag{48}$$

where $\underline{\underline{\mathbf{R}}}$ is the rate of deformation tensor:

$$\underline{\underline{\mathbf{R}}} = \frac{1}{2}\left(\nabla V + \nabla V^T\right) \tag{49}$$

and C_{av} is an artificial viscosity coefficient applied under compression deformation rates only:

$$C_{av} = 0 \text{ for } tr(\underline{\underline{\mathbf{R}}}^2) > 0; C_{av} = 0.0133 s^2 \text{ otherwise.} \tag{50}$$

A comparison between numerical and analytical solutions, showing reasonable agreement, can be seen in Figures 4 to 7. These results are comparable, although a bit more diffusive, to those obtained in [7] with a more restricted approach. Although more work may be needed in the selection of weight and shape functions, the simple ones chosen in this work have shown to be adequate for dealing with a complex nonlinear problem involving all aspects of the thermodynamic of the flow.

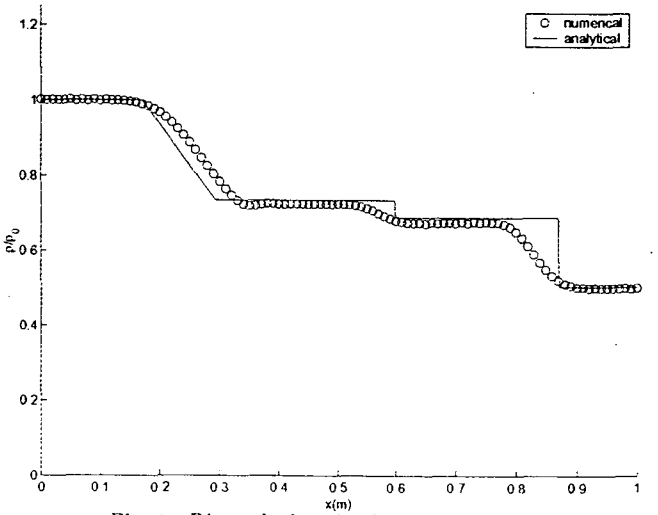

Fig. 4. Dimensionless density at $t = 0.001\ s$.

VI. Conclusions

A general Bond Graph approach for Computational Fluid Dynamics (BG-CFD), developed in previous papers by the authors, has been applied to one-dimensional compressible flow problems. Piecewise constant shape functions and piecewise linear weight functions were used for the density and the entropy, while

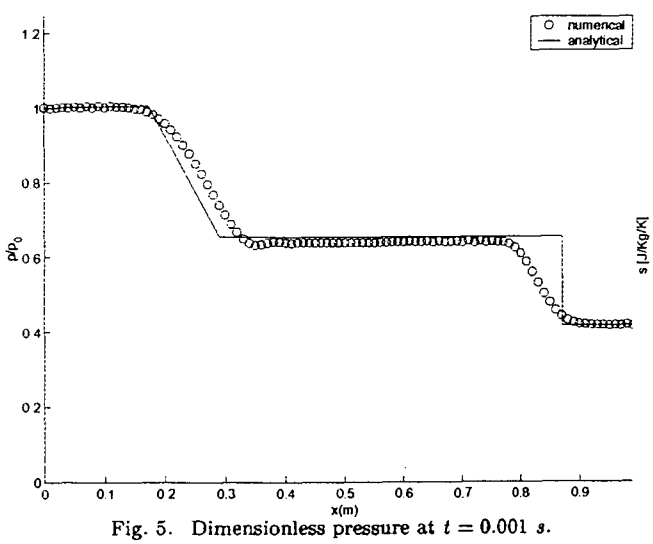

Fig. 5. Dimensionless pressure at $t = 0.001$ s.

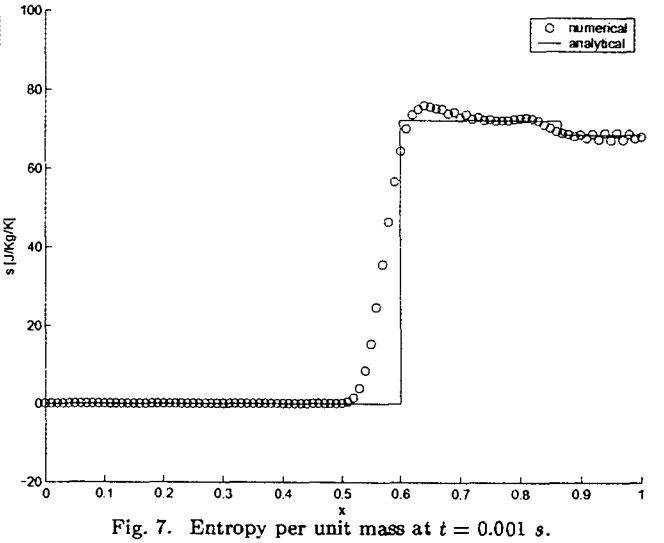

Fig. 7. Entropy per unit mass at $t = 0.001$ s.

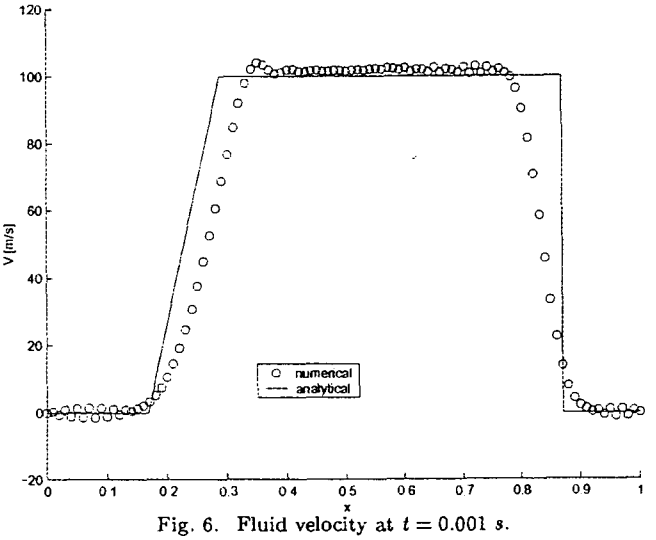

Fig. 6. Fluid velocity at $t = 0.001$ s.

piecewise linear shape functions were used for the flow velocity. Upwinding was applied to the entropy equation through a velocity-dependent entropy weight function. The shock tube problem has been modeled and simulated, and the results have been compared against the available analytical solution. The numerical simulation shows that, even with the simple shape and weight functions selected for this case, the BG-CFD approach is able to deal with really complex non-linear flow problems in which all the thermodynamic aspects are taken into account. The accuracy of the model may be surely increased in the future by selecting more complex shape and weight functions.

Acknowledgments

E. F. Gandolfo wishes to thank FOMEC (Fondo para el Mejoramiento de la Calidad Universitaria) for the financial support obtained to accomplish this work. J. L. Baliño wishes to thank Conselho Nacional de Desenvolvimento Científico e Tecnológico (CNPq, Brazil) for the financial support as Visiting Researcher at IPEN.

References

[1] Karnopp D.C., Margolis D.L. & Rosenberg R.C., System Dynamics: a Unified Approach, 2nd Ed., Wiley Interscience, ISBN 0-471-62171-4, 1990.

[2] Baliño, J. L., Larreteguy, A. E. & Gandolfo, E. F., A General Bond Graph Approach for Computational Fluid Dynamics. Part I: Theory, *ICBGM '2001*, The Society for Computer Simulation, pp. 41-46. ISBN 1-56555-221-0, 2001.

[3] Baliño, J. L., Larreteguy, A. E. & Gandolfo, E. F., A General Bond Graph Approach for Computational Fluid Dynamics, submitted to *Mathematics and Computers in Simulation*.

[4] Gandolfo, E. F., Larreteguy, A. E. & Baliño, J. L., A General Bond Graph Approach for Computational Fluid Dynamics. Part II: Applications, *ICBGM '2001*, The Society for Computer Simulation, pp. 47-52. ISBN 1-56555-221-0, 2001.

[5] Gandolfo, E. F., Larreteguy, A. E. & Baliño, J. L., Bond Graph Modeling of Fluid Convection-Diffusion Problems, submitted to *Mathematics and Computers in Simulation*.

[6] Baliño, J. L., Bond-Graph Approach for Computational Fluid Dynamics: a Comparison with other Numerical Methods, submitted to this Conference.

[7] Fahrenthold E.P., Venkataraman M., Eulerian Bond Graphs for Fluid Continuum Dynamic Modeling, *Transactions of the ASME*, Vol. 118, pp. 48-57, 1996

[8] Emanuel G., Gasdynamics: Theory and Applications, *AIAA Education Series*, New York, 1986.

[9] Sod G.A., A Survey of Several Finite Difference Methods for Systems of Nonlinear Hyperbolic Conservation Laws, *Journal of Computational Physics*, Vol. 27, pp. 1-37, 1978.

[10] Monaghan J.J., Gingold R.A., Shock Simulation by the Particle Method SPH, *Journal of Computational Physics*, Vol. 52, pp. 374-389, 1983.

CENTRO DE ENGENHARIA NUCLEAR

TERMO-HIDRÁULICA E ANÁLISE DE ACIDENTES CENT

Bond-Graph Modeling of 1-D Compressible Flows

(Anais do Second IEEE International Conference on System, Man and Cybernetics, SMC02: 6-9 Outubro / 2002)

Artigo Científico
P&D.CENT.CENT.018
ARTC.012.00

AUTOR	Rubrica	Data	VERIFICADOR	Rubrica	Data
Jorge Luis Baliño		19/11/02			

APROVAÇÕES		Rubrica	Data
Chefe de Área	Benedito Dias Baptista Filho		22/11/02
Lider	Benedito Dias Baptista Filho		22/11/02
Gerente do Centro	Antonio Teixeira e Silva		25/11/02

ARQUIVO			

TC

repetida

IPEN/CNEN-SP
BIBLIOTECA
"TEREZINE ARANTES FERRAZ"

Formulário de envio de trabalhos produzidos pelos pesquisadores do IPEN para inclusão na Produção Técnico Científica

---

AUTOR(ES) DO TRABALHO:
Gandolfo, E.F.; Lavieteguy, A.E; Zolezzi, J.L.

LOTAÇÃO: CENT RAMAL: 9227

TIPO DE REGISTRO:

art. / periód.:	☐	Publ. IPEN	☐	. resumo	☐
cap. de livro	☐	Art. conf	☑	outros (folheto, relatório, etc...)	☐

TITULO DO TRABALHO:
Bond - graph Modeling of 1-D Compressible Flows

APRESENTADO EM: (informar os dados completos - no caso de artigos de conf., informar o título da conferência, local, data, organizador, etc..)
2nd IEEE International Conference on System, Man and Cybernetics SMC02 6-9/10/02

SMC'02

PALAVRAS CHAVES PARA IDENTIFICAR O TRABALHO:
Bond graphs, Computational Fluid Dynamics, compressible flow, shock tube

ASSINATURA: Gandolfo

DATA: 14/12/02

3582